

## Funding Disclosures

Under the mentorship of Dr. Chamith Rajapakse, Trenton Campos lead this research project with funding from the Class of 1971 Robert J. Holtz Fund Grant.

## Abstract

The primary objective is to create biodegradable scaffolds to be implanted in patients that suffer severe bone-related traumas or require orthopaedic implants. In order to do this with bioprinting, we must be able to create a print with osteogenic properties, sufficient structural integrity, and the capability to be vascularized in the future. We seek to fulfill the first two objectives by creating a PCL:HA scaffold framework. The polycaprolactone (PCL) provides structural integrity, while the hydroxyapatite (HA) promotes bone growth as it degrades. In order to overcome the dangers associated with previous methods, we will be utilizing a new PCL printing methodology that involves quantitative melting of the PCL and mixing in the HA. We will be evaluating our scaffolds' biomechanical properties by conducting a compression test. We will then compare the different stiffness (N/mm) of varying compositions of PCL:HA in addition to the stiffness of different scaffold geometries. This data will be utilized to determine the optimal scaffold for the biodegradable implants. Afterward, the methodology will be utilized for printing in surgical applications, such as spinal fusion surgeries.

## Introduction

Traumatic bone injuries often require interventional measures in the form of bone stents. Other types of orthopaedic interventions, such as spine cages, frequently require metal implants that differ from the properties of bone. Recent developments in bioprinting and biocompatible printing materials make bioprinting a promising method for designing biodegradable scaffolds for these purposes. In order to function as an interventional measure for bone injuries or bone-related procedures, a print must have sufficient structural integrity, promote bone growth, and have the capability to be vascularized.

Our goal was to create the optimal scaffolds for various surgical procedures. The most popular materials used in the fabrication of bone stents are polycaprolactone (PCL) and hydroxyapatite (HA). The PCL provides structural integrity and the HA has osteogenic properties as it is slowly dissolved within the body.

Current methods printing methods are cytotoxic and expensive as they dissolve the PCL and HA using solvents such as chloroform to make the bioink sufficiently uniform and viscous for extrusion printing.

We decided to use a different methodology in our printing approach that forgoes the use of solvents by quantitatively melting the PCL and mixing in the HA.

## Methods - Scaffolds

Molecular weight 45,000 g PCL pellets and 10  $\mu$ m HA powder were used. Dry PCL:HA mixtures were created using varying weight ratios of PCL to HA ranging from 90:10 to 65:35. Compositions were varied at 5% increments. Prior to printing, each mixture was melted in the extruder nozzle and mixed thoroughly to ensure proper dispersion of the HA. The pneumatic extruder nozzle was then placed into the bioprinter. For each composition, four sets of cuboids were printed with varied infill distances (3 and 5 mm) and geometries (grid and triangle). (Figure 1). For each set, two 10 x 10 x 5 mm<sup>3</sup> cuboids were printed. Print speed, pressure (PSI), print surface, and layer height were held constant. The increased concentrations of HA resulted in increased bioink viscosity and the temperature was increased to standardize viscosity.

### Scaffold Infill Distances and Geometries

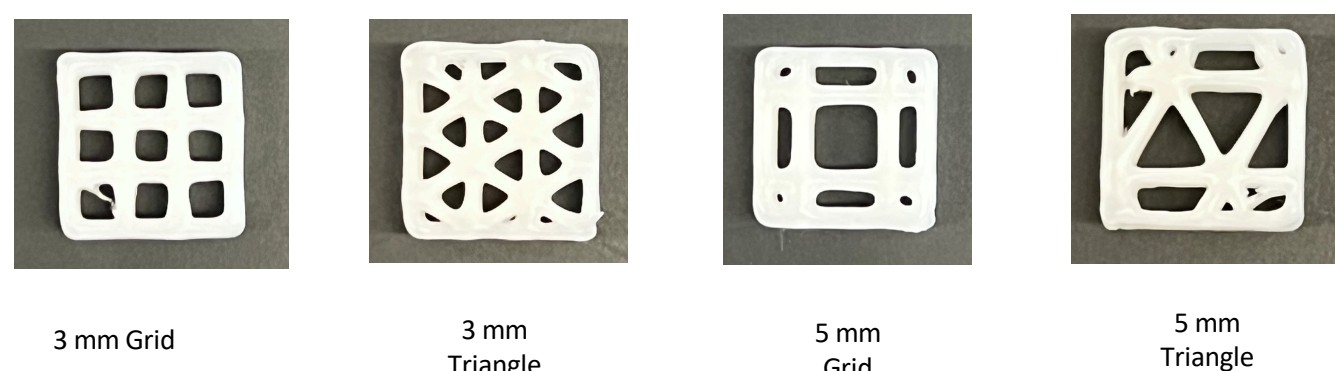


**Figure 1.** Depicts the four different sets of prints. Infill distances were varied from 3 to 5 mm and geometries were varied from grid to triangle.

## Methods – Stress Testing

### Biomechanical Testing

Biomechanical properties were accessed for each scaffold using a compression test, which yielded stiffness (N/mm). The machine used for the test was the Instron 8874. The scaffolds were compressed in a manner where the face of the cube as depicted in Figure 1 made contact with the Instron.

The scaffolds would be analyzed to determine the strongest PCL:HA concentration and the strongest scaffold type.

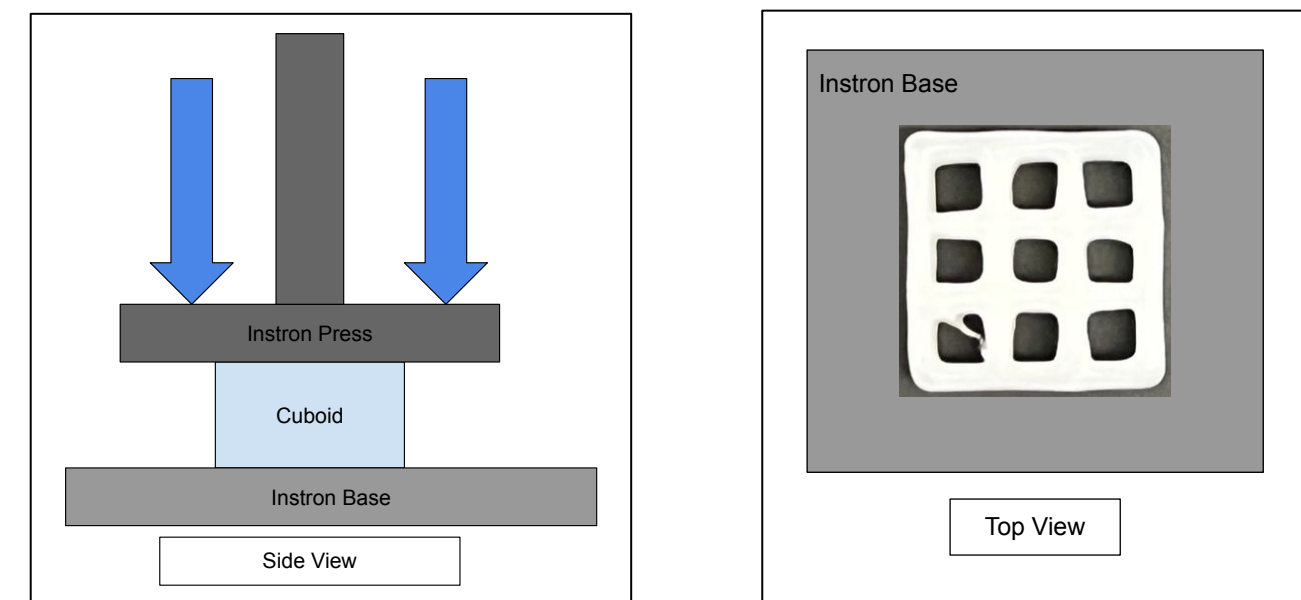


**Figure 3.** The picture on the left depicts the side profile of the Instron machine during the biomechanical testing. The figure on the right depicts the top view of the Instron machine (excluding the press). Note how the face of the cube as depicted in Figure 1 lies flat on the Instron base.

### ANOVA Analysis

In order to determine if there was a statistically significant difference between the different scaffold types, ANOVA testing was used.

Due to the small samples size resulting from the fact that two cubes were tested for each scaffold type at a concentration, the data was grouped according strictly to scaffold type.

## Results & Discussion – Biomechanical Testing of PCL:HA Concentration

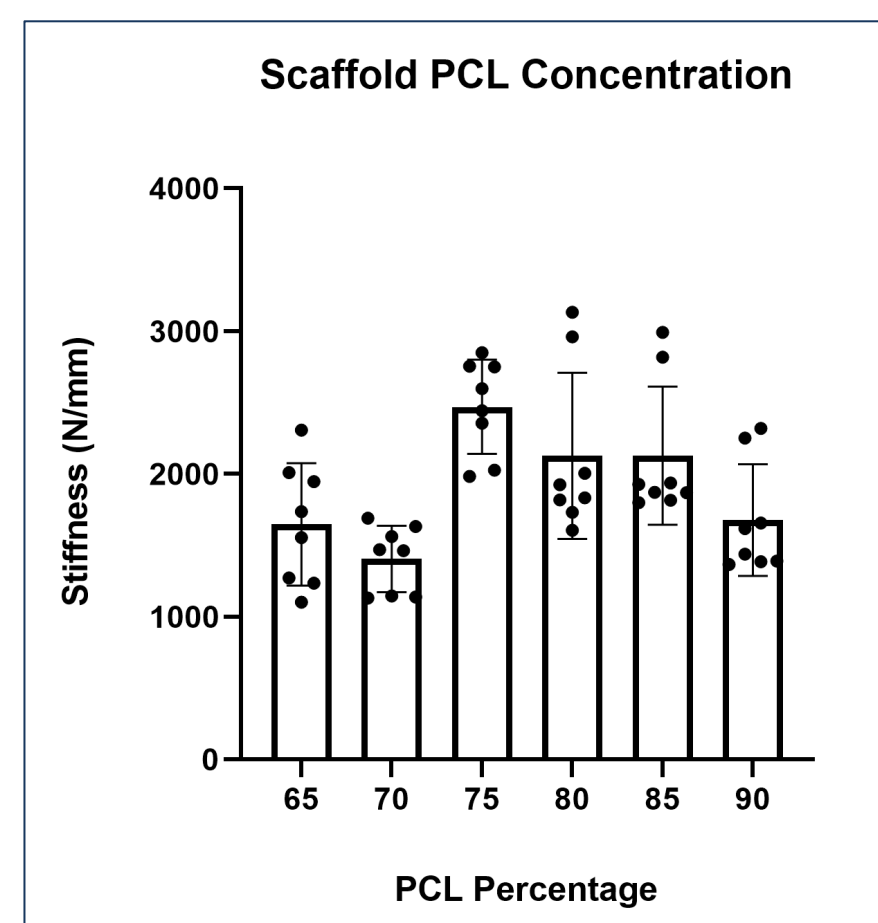


**Figure 4.** Depicts the average stiffness of the different scaffold compositions in addition to the upper and lower quartiles. The graph shows how the 75:25 composition had the greatest average stiffness.

Compositions of PCL:HA were uniformly printed up to ratios of 65:35. There was no decrease in cuboid quality as the HA concentration was increased; however, a small reduction in thickness was noted, likely due to the increased viscosity of the prints. Compression testing showed that print compositions of 75:25 had the greatest stiffness, with a mean maximal load of 2470 N/mm<sup>2</sup>. Due to a small sample size, further testing is necessary.

## Results & Discussion – Biomechanical Testing of Scaffold Type

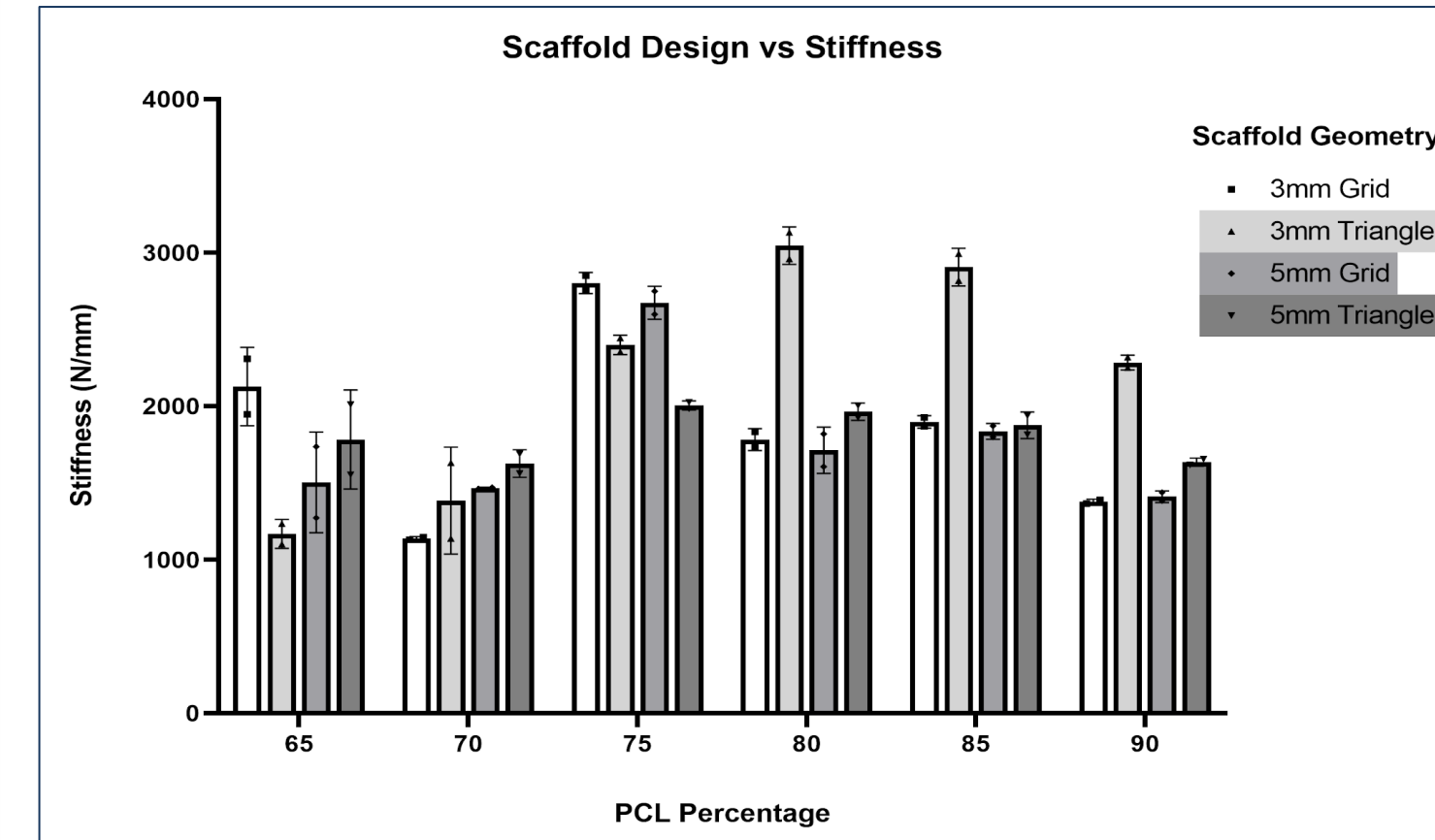


**Figure 5.** Depicts the different scaffold concentrations and their stiffnesses. The graph is further subdivided to show the four different sets of prints for each composition. As shown, 75:25 has the greatest average strength. The graph shows there are no significant differences between the strengths of the different geometries. This was proved with ANOVA testing.

ANOVA testing showed that there were no statistically significant differences between the stiffness of different infill geometries and lengths. The calculated P-Value was 0.1944, which is above the alpha value of 0.05. The results we obtained fail to show that the difference between the strengths of different scaffolds is caused by anything other than chance.

It should be noted that in the experimental design, the scaffolds were compressed in a way that the Instron made contact with the faces of the cubes depicted in Figure 1. Because the scaffolds were compressed in this manner, the difference between grid and triangle geometries likely had no effect.

## Applications – Spine Cages

Our developed methodology was then utilized to create spinal cages for use in TLIF spinal fusion procedures. We opted to utilize 80:20 PCL:HA ratios as it was easier to print with, even though stress testing showed it yielded lower stiffness values. We used CAD software to design several different spinal cage prototypes as shown in Figure 6. We then elected to go with the scaffolds shown in Figure 7 as their small size fit better with the TLIF procedure. Furthermore, they are similar in design to common TLIF cages on the market. 10 copies of three different infill geometries (3 mm grid, 4 mm grid, 4 mm ZigZag) were printed in order to build up a substantial sample size for mechanical testing. The mechanical testing revealed that the 3mm-grid design produced the strongest spinal cage, with the highest stiffness (4420 +/- 186.9 N/mm) and yield force (2672 +/- 164.2 N) values. Because of these superior mechanical properties, the 3mm-grid spinal cage is likely the best suited for use in TLIF procedures, given its ability to handle high-magnitude compressive forces like those in the spine. Furthermore, the elastic modulus of our PCL:HA blend (255.9 +/- 34.35 MPa) is much closer to the modulus of human trabecular bone (120-450 MPa) (1) when compared to titanium cages which are often in the range of 100 GPa. These scaffolds more closely resemble the modulus of bone and act as fully synthetic spine cages as a result of the HA.



**Figure 6.** Initial Prototypes of Spine Cages

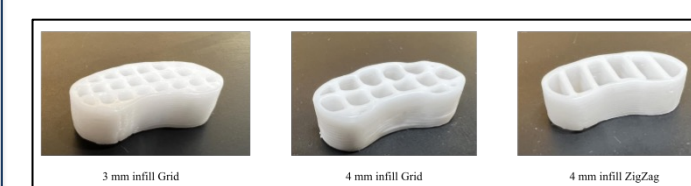


**Figure 7.** The 3 different infill geometries created for the optimal scaffold

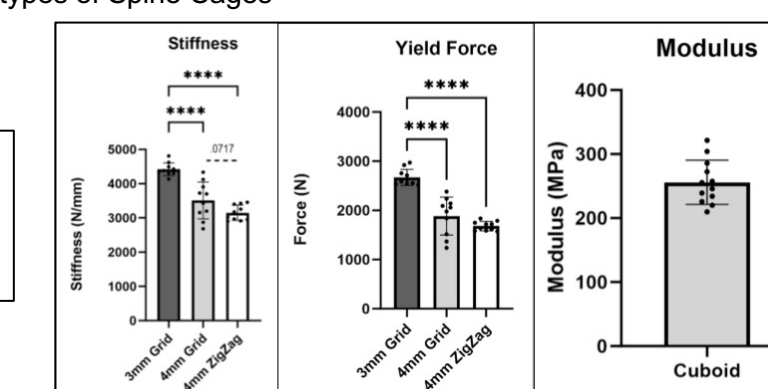


**Figure 8.** Data collected from different scaffold geometries

## Applications – Image Based Scaffolds

For image-based applications, we attempted to recreate hard and soft tissue based on medical imaging. Medical DICOM files were converted into STL files and then printed into PCL:HA scaffolds utilizing our printing methodology.

As initial applications of this method, femur segments were recreated to showcase our capabilities to model hard tissue and spinal discs were recreated for the soft tissue model. Both the femur and disc segments were bioprinted utilizing PCL:HA ratios of 80:20 for ease of manufacturing.

For the hard tissue models, DICOM files are converted directly into STL files utilizing the software 3D Slicer. The software allows for direct segmentation of the imaging to print a certain specified section of hard tissue. For soft tissue models, we developed a protocol called negative imaging to generate soft tissue models based on hard tissue imaging. This method is employed due to the difficulty of isolating soft tissue, such as spinal discs, in DICOM files without contrast enhancement. The protocol utilizes CAD to generate a mold of the soft tissue from the surrounding hard tissue. The mold is then cleaned in Meshmixer to fix any imperfections.

Due to the precision of these models, they can also be utilized as image-based, implantable biological scaffolds for musculoskeletal applications.

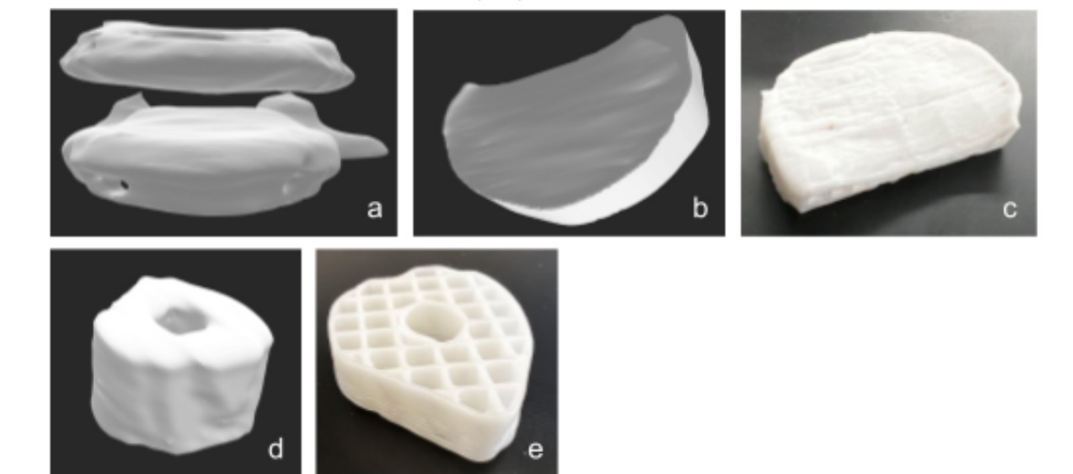


**Figure 9.** (a) STL file of patient's L2 and L3 vertebrae, (b) STL of L2-3 disc, (c) 3D printed spine disc, (d) STL of femur segment, (e) 3D printed femur segment

## Conclusion

Melting dry mixtures of PCL with subsequent HA mixing is a better alternative than the utilization of chloroform to dissolve the PCL. Higher compositions of HA can be obtained and the method is much safer, cost-effective, and less time-consuming. Furthermore, melting the PCL allows printing to be quickly resumed in contrast to having to redissolve the PCL in chloroform with the alternative method. Further research is needed to investigate the osteogenic and mechanical properties of the newly created PCL:HA prints and determine the optimal concentration for different orthopaedic applications. Likewise, experiments should be designed so that the scaffold geometries have a more direct role in compression testing by having the scaffold geometries be in the plane of compression. Interestingly, while no change was noted for the different geometries in the cuboids, there was a significant difference between the different scaffold geometries for the spine cages. This could potentially stem from having a larger sample size and further testing needs to be conducted in regard to this.

This project worked to establish the best scaffolding for bioprinted bone stents and other applications that require orthopedic implants. The next stage of the process is to be able to vascularize our scaffolds. However, due to the hydrophobic nature of PCL, it is very difficult to vascularize the PCL itself.

Our proposed methodology to combat this is to encapsulate a hydrogel within the geometry of our scaffolds. The proposed hydrogel will be made up of sodium alginate and GelMA and will have double-factor crosslinking. We will vascularize cells within this hydrogel medium to act as a fully functioning bone stent. With our proposed methodology, the PCL:HA will provide structural integrity and promote bone growth, while our hybrid hydrogel within the scaffold will be vascularized to function like a true bone stent.

The methodology has already been created to make custom-fit, image-based biodegradable scaffolds and we already have a mechanically relevant spine cage design. Once vascularization is complete, we will have scaffolds that would have the potential to be used in surgical practice and that may be superior to current orthopaedic implants.

## References

- 1) Kang, H, et al, J Biomech Eng, 2013.